Available online at http://scik.org

J. Math. Comput. Sci. 11 (2021), No. 2, 1904-1921

https://doi.org/10.28919/jmcs/5423

ISSN: 1927-5307

EFFECT OF EXTERNALLY APPLIED TRANSVERSE MAGNETIC FIELD ON BLOOD FLOW IN TAPERED STENOSED ARTERY: BY FROBENIUS METHOD

B. S. VEENA*, ARUNDHATI WARKE

Symbiosis Institute of Technology (SIT), Symbiosis International (Deemed University), Lavale, Pune - 412 115

Maharashtra State, India

Copyright © 2021 the author(s). This is an open access article distributed under the Creative Commons Attribution License, which permits unrestricted use, distribution, and reproduction in any medium, provided the original work is properly cited.

Abstract: A mathematical model to observe the behaviour of blood flow in the presence of externally applied transverse magnetic field in a tapered stenosed artery is developed. Blood flow is assumed to follow Bingham plastic model. The effect of constant and variable viscosity on blood flow has been studied. To find expressions for important flow characteristics; volumetric flow rate, radial velocity and wall shear stress, the system of non-linear differential equations is solved by Frobenius method. Matlab 10.7.0 is used to analyze the behavior of blood flow. It is observed that these important flow characteristics change their behavior in stenosed tapered artery and externally applied transverse magnetic field helps in regulating these changes up to some extent.

Keywords: viscosity; magnetic field; blood flow; Frobenius method; stenosis; Bingham-plastic.

2010 AMS Subject Classification: 35N05, 76W05.

1. INTRODUCTION

Cardiovascular diseases are one of the main causes of death in both developed and developing countries. Atherosclerosis is a type of arterial disease, which is due to cholesterol plaque in inner

*Corresponding author

E-mail address: veena@sitpune.edu.in

Received January 13, 2021

wall of the artery. This narrows the artery passage and a loss of elasticity in the artery. Modeling and analysis of hemodynamic of human vascular system improve our understanding of vascular disease and provide valuable insights, which can help in the development of efficient treatment methods. Stenosis is the partial occlusion of blood vessels, which carries blood to heart. Because of this partial occlusion, the blood supply to the heart suffers; as a result, there will be changes in blood pressure, which causes heart diseases.

Magnetohydrodynamics is the study of magnetic properties of electrically conducting fluid. In 1840, an experimental study of flow in capillaries has been conducted by the French physician Poiseuille and is well-known as Poiseuille's flow. Later, in last two decades, lot of research has been carried out on blood flow dynamics under the influence of magnetic field. In particular, the study of flow of blood in stenosed arteries under the influence of magnetic field has been carried out with various perspectives by developing / modifying mathematical models. The first Blood Flow Dynamic (BFD) model was developed mathematically by Haik and is further extended by Tzirtzilakis and Kafoussias in 2001. Since then, many researchers have developed/modified many mathematical models [1–4]. It is reported that the normal flow changes to disturbed flow in presence of stenosis, resulting into atherosclerosis [5]. The effect of magnetization on blood flow in mild stenosed artery in the presence of erythrocytes through an intended tube is discussed by developing a mathematical model using Frobenius method [6, 7]. The stress increases significantly with increase in magnetization. Increase in pressure gradient corresponds to the increase in both magnetic field and hematocrit but the increase in magnetic field is more substantial than that of hematocrit [8, 9]. Around the turn of 20^{th} century, it has been observed that blood exhibits non-Newtonian behavior and because of complexity of problem, it is concluded that unsteady state non-Newtonian blood flow can be modeled only by higher order equations [10–12]. Externally applied transverse magnetic field of different intensities on time dependent blood flow model in non-tapered artery affects all the flow characteristics in multi stenosed artery. It is also observed that, wall shear stress increases, flow pattern changes in non-Newtonian rheology, as compared to the results of Newtonian rheology [13]. A pulsatile flow 3D model of human aorta at different stages of atherosclerosis is studied by considering 50% and 80% stenosis to the healthy aorta geometry, found that the wall shear stress distribution and magnitude are strongly affected by size of stenosis, its features and location [14, 15].

This paper deals with pulsatile flow of blood in presence of externally applied transverse magnetic field through a tapered stenosed artery. Two cases are considered, a) blood viscosity is constant

and b) blood viscosity varying with shear stress (depends on hematocrit and position). The non-linear differential equations governing the fluid flow are solved using Frobenius method and the expressions for velocity, flow rate and shear stress are obtained. This study is useful to regulate blood flow in tapered stenosed artery.

2. PROBLEM FORMULATION

The schematic diagram of tapered stenosed artery with tapering angle φ is as shown in Fig. 1. If $\varphi < 0$ then the artery is converging, if $\varphi > 0$ then diverging, and if $\varphi = 0$ then the artery is non-tapered.

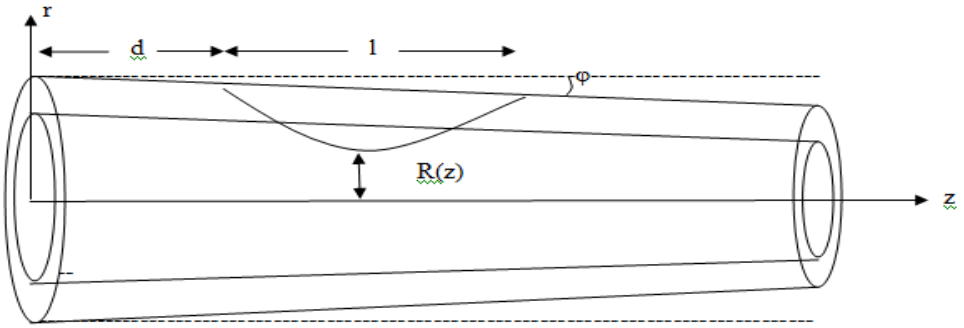

Fig. 1. Schematic representation of stenosed tapered artery with tapering angle φ

The mathematical model of tapered stenosed artery is given by the equation

$$R(z)=\begin{cases}(R_0+md)+\left[m-\dfrac{h}{l}\right](z-d)+\left(\dfrac{h}{l^2}\right)(z-d)^2, \text{if } d\le z\le d+l\\ (mz+R_0), \text{ otherwise}\end{cases} \tag{1}$$

where φ is the tapering angle, $m = \tan\ \varphi$, $h = 4x0.4\ R_o \sec\ \varphi$ = height of stenosis, R_o is radius of non-stenosed part, $R(z)$ is radius of stenosed part, l is length of stenosis d is starting point of stenosis and z is axial coordinate [16].

The problem is formulated by assuming the blood flow as unsteady, laminar and fully developed pulsatile flow, blood is incompressible and transverse magnetic field is applied externally with negligible electric field.

The governing equation satisfying the above conditions is

$$-\frac{\partial P}{\partial z}+\frac{1}{r}\frac{\partial}{\partial r}(r\tau)+kM\frac{dH}{dz}=\rho\frac{du}{dT} \tag{2}$$

where P is pressure, z is axial coordinate, r is radial coordinate, k is permeability, M is magnetization, τ is shear stress, ρ is density, u is axial velocity and T is time parameter.

Blood is assumed to be non-Newtonian, and it follows Bingham plastic fluid model,

$$\text{i.e.:}\quad \tau = \tau_0 + \mu\left(-\frac{\partial u}{\partial r}\right) \tag{3}$$

Here τ_0 is yield stress and μ is viscosity.

Boundary conditions are

$$u = 0 \quad \text{at} \quad r = R(z) \text{ and } \frac{\partial u}{\partial r} = 0 \quad \text{at} \quad r = 0 \tag{4}$$

The following radial coordinate transformations are used:'

$$y = \frac{r}{R_0} \quad \text{at} \quad t = \frac{T}{t_0} \tag{5}$$

where R_0 is length and t_0 is time scaling parameter. Then (2) becomes

$$-\frac{\partial P}{\partial z} + \frac{1}{yR_0}\frac{\partial}{\partial y}(y\tau) + kM\frac{dH}{dz} = \frac{\rho}{t_0}\frac{du}{dt} \tag{6}$$

and (3) becomes

$$\tau = \tau_0 + \frac{\mu}{R_0}\left(-\frac{\partial u}{\partial r}\right) \tag{7}$$

Boundary conditions becomes

$$u = 0 \quad \text{at} \quad y = \frac{R(z)}{R_0} \quad \text{and} \quad \frac{\partial u}{\partial y} = 0 \quad \text{at} \quad y = 0 \tag{8}$$

So using (7), equation (6) becomes

$$\frac{1}{y}\frac{\partial}{\partial y}\left\{y\tau_0 + \frac{\mu y}{R_0}\left(-\frac{\partial u}{\partial y}\right)\right\} = \frac{\rho R_0}{t_0}\frac{du}{dt} - kMR_0\frac{dH}{dz} + R_0\frac{dP}{dz}. \tag{9}$$

In general, viscosity of blood is not constant in diseased condition; it is assumed that viscosity varies with radial coordinate and hematocrit. Einstein's formula is used to find variable viscosity:

$$\mu = \mu_0\left[1 + \beta\hbar(r)\right], \tag{10}$$

Here β is a constant whose value is 2.5 for blood, μ is viscosity of blood, μ_0 is viscosity of

plasma and $h(r)$ is given by the formula

$$h(r) = He\left[1-\left(\frac{r}{R_0}\right)^n\right] = He\left[1-y^n\right] \tag{11}$$

where He is hematocrit value and n is the parameter determining the shape of flow.

Using (10) in equation (9), we get,

$$\frac{1}{y}\frac{\partial}{\partial y}\left[\left(A-By^n\right)y\mu_0\left(-\frac{\partial u}{\partial y}\right)\right] = \frac{\rho R_0^2}{t_0}\frac{du}{dt} - kMR_0^2\frac{dH}{dz} + R_0^2\frac{dP}{dz} - \frac{R_0\tau_0}{y} \tag{12}$$

where $A = 1+\beta He$ and $B = \beta He$.

As the flow is pulsatile, $u(y,t) = U(y)e^{jwt}$ (13)

$$\frac{\partial u}{\partial y} = U'(y)e^{jwt} \quad \text{and} \quad \frac{\partial u}{\partial t} = U(y)\,jwe^{jwt} \tag{14}$$

Using (13) and (14) in (12),

$$\frac{1}{y}\frac{\partial}{\partial y}\left[\left(A-By^n\right)y\frac{\partial U}{\partial y}\right] + j\alpha^2 U = \left(\frac{Da^2MR_0^4}{\mu_0}\frac{dH}{dz} - \frac{R_0^2}{\mu_0}\frac{dP}{dz} + \frac{R_0\tau_0}{y\mu_0}\right)e^{-jwt} \tag{15}$$

where $j = \sqrt{-1}$ and $Da^2 = \frac{k}{R_0^2}$ and $\alpha^2 = \frac{\rho R_0^2}{t_0\mu_0}w$ (16)

The important force for blood to flow is local pressure gradient which depends on heart pressure pulse and is periodic in nature. Hence, it is assumed that $\frac{R_0^2}{\mu_0}\frac{\partial P}{\partial z} = ce^{jwt}$, where $w = 2\pi f$, f is pulse frequency and c is amplitude of pulsatile flow. Hence (15) becomes

$$\left(A-By^n\right)\frac{\partial^2 U}{\partial y^2} + \frac{1}{y}\left(A-By^n\right)\frac{\partial U}{\partial y} - Bny^{n-1}\frac{\partial U}{\partial y} + j\alpha^2 U = RHS, \tag{17}$$

where $RHS = \left(\frac{Da^2MR_0^4}{\mu_0}\frac{dH}{dz}e^{-jwt} - c + \frac{R_0\tau_0}{y\mu_0}e^{-jwt}\right)$

Let us denote $\left(A-By^n\right)\frac{\partial^2 U}{\partial y^2} + \frac{1}{y}\left(A-By^n\right)\frac{\partial U}{\partial y} - Bny^{n-1}\frac{\partial U}{\partial y} + j\alpha^2 U$ by LHS.

3. SOLUTION USING FROBENIUS METHOD

Frobenius method is used to solve equation (17) and for this, U must be bounded at $y = 0$. Therefore, the only admissible solution is

$$U = l\sum_{0}^{\infty} A_i y^i + \frac{RHS}{4A}\sum_{0}^{\infty} B_i y^{i+2?} \tag{18}$$

where A_i and B_i are series constants, l is arbitrary constant to be determined using boundary conditions. Here $l\sum_{0}^{\infty} A_i y^i$ is the solution of homogeneous part, and $\frac{RHS}{4A}\sum_{0}^{\infty} B_i y^{i+2?}$ is the solution of non-homogeneous part of (17).

Using no slip condition $U = 0$ at $y = \frac{R(z)}{R_0}$, we get

$$l = -\frac{RHS}{4A}\frac{\sum_0^{\infty} B_i y^{i+2}}{\sum_0^{\infty} A_i y^i} \tag{19}$$

$$\text{i.e., } l = -\frac{RHS}{4A}\frac{\sum_0^{\infty} B_i \left(\frac{R(z)}{R_0}\right)^{i+2?}}{\sum_0^{\infty} A_i \left(\frac{R(z)}{R_0}\right)^{i}}. \tag{20}$$

Solution of homogeneous part:

Using U, $\frac{dU}{dy}$ and $\frac{d^2U}{dy^2}$ in LHS of (17), we get

$$A\sum_{0}^{\infty} i(i-1)A_i y^{i-2} - B\sum_{0}^{\infty} i(i-1)A_i y^{i+n-2} +$$

$$+A\sum_{0}^{\infty} A_i i y^{i-2} - B\sum_{0}^{\infty} A_i i y^{i-2+n} - B\sum_{0}^{\infty} A_i i n y^{i+n-2} + j\alpha^2\sum_{0}^{\infty} A_i y^i = 0\ . \tag{21}$$

Comparing the coefficients of y^{i+1}, we get

$$A_{i+3} = [\left[BA_{i-n+3}(i-n+3)(i+3) - j\alpha^2 A_{i+1} \right] / A(i+3)^2 \quad (22)$$

Solution of non-homogeneous part:

Using U, $\frac{dU}{dy}$ and $\frac{d^2U}{dy^2}$ in (17), we get,

$$\left(A - By^n\right)\frac{RHS}{4A}\sum_0^\infty B_i(i+2)(i+1)y^i + \frac{1}{y}\left(A - By^n\right)\frac{RHS}{4A}\sum_0^\infty B_i(i+2)y^{i+1} -$$

$$-Bny^{n-1}\frac{RHS}{4A}\sum_0^\infty B_i(i+2)y^{i+1} + j\alpha^2\frac{RHS}{4A}\sum_0^\infty B_i y^{i+2} = RHS \quad (23)$$

Comparing the coefficients of y^{i-1}, we get

$$B_{i-1} = \left[BB_{i-n-1}(i-n+1)(i+1) - j\alpha^2 B_{i-3} \right] / A(i+1)^2 \quad (24)$$

Hence,

$$A_{i+1} = [\left[BA_{i-n+1}(i-n+1)(i+1) - j\alpha^2 A_{i-1} \right] / A(i+1)^2, \quad (25)$$

$$B_{i+1} = \left[BB_{i-n+1}(i-n+3)(i+3) - j\alpha^2 B_{i-1} \right] / A(i+3)^2 \quad (26)$$

with $A_0 = B_0 = 1$ and $A_{-m} = B_{-m} = 0$.

4. RESULTS AND DISCUSSION

The list of parameters and their corresponding values used for simulation is given in the Table 1. As the flow is pulsatile, the flow characteristics are in the form of imaginary numbers. So, to observe the profile of these important flow characteristics, only real part is considered.

Table 1. Value of parameters for simulation

Parameter	Value	Parameter	Value
μ	0.0035 Pa.s	R_0	0.0025 m
u_0	0.36 m/s	k	1
H_0	0.2 Tesla	μ_0	0.0018 Pa.s
M	200 amp/m	ρ	1060 kg/m^3
f	0.2 Hz	l	0.05 m
d	0.02 m	t_0	100 s
$\left(\frac{dp}{dz}\right)_0$	3447 P	n	2

Axial velocity

Substituting the value of l in (18), we get,

$$u = \left[-\frac{\frac{RHS}{4A}\left[\sum_0^\infty B_i \left(\frac{R(z)}{R_0}\right)^{i+2?} \sum_0^\infty A_i y^i - \sum_0^\infty A_i \left(\frac{R(z)}{R_0}\right)^i \sum_0^\infty B_i y^{i+2}\right]}{\sum_0^\infty A_i \left(\frac{R(z)}{R_0}\right)^i} \right] e^{jwt} \tag{27}$$

$$\bar{u} = \frac{\left[-\frac{\frac{RHS}{4A}\left[\sum_0^\infty B_i \left(\frac{R(z)}{R_0}\right)^{i+2?} \sum_0^\infty A_i y^i - \sum_0^\infty A_i \left(\frac{R(z)}{R_0}\right)^i \sum_0^\infty B_i y^{i+2}\right]}{\sum_0^\infty A_i \left(\frac{R(z)}{R_0}\right)^i} \right] e^{jwt}}{-\frac{R_0^2}{8\mu_0}\left(\frac{dp}{dz}\right)_0} \tag{28}$$

where $u_0 = -\frac{R_0^2}{8\mu_0}\left(\frac{dp}{dz}\right)_0$ is the average velocity with $\left(\frac{dp}{dz}\right)_0$ as pressure gradient in non-stenosed artery in the absence of magnetic field.

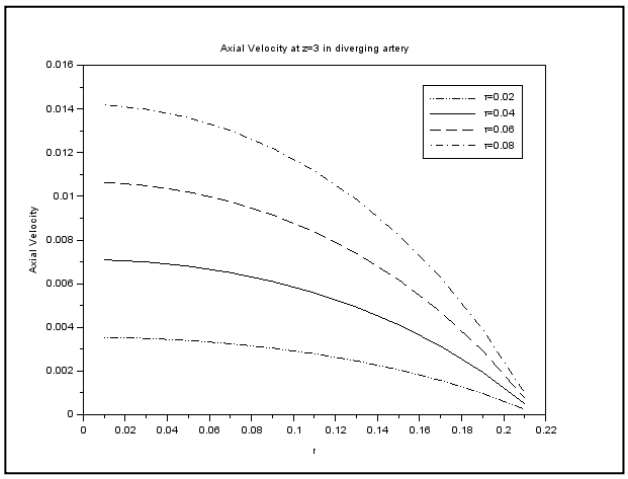

Fig. 2. Axial velocity for different yield stress at $z = 3$ in diverging artery.

Fig. 2 shows the profile of axial velocity at $z = 3$ in diverging artery for different yield stress by keeping remaining parameters constant. Here, angle of tapering is considered as 0.01. Hence the radius of artery at z=3 is 0.2159978. It is observed from the figure that rise in yield stress will help in elevating axial velocity, but at the same time rate of decrease in axial velocity increases.

Table 2. Axial velocity for different tapering angles at $z = 4$

r	φ =0.02	φ =0.015	φ =0.01	φ =-0.01	φ =-0.015	φ =-0.02
$\boldsymbol{R(z)}$	0.2339915	0.2139937	0.1939965	0.1139939	0.0939847	0.0739701
0.01	0.0080831	0.0065688	0.0052689	0.0016998	0.0011403	0.0006961
0.03	0.0079976	0.006480	0.0051773	0.0016005	0.0010399	0.0005947
0.05	0.0078245	0.0063003	0.0049920	0.0013998	0.0008367	0.0003896
0.07	0.0075597	0.0060255	0.0047086	0.0010926	0.0005258	0.0000758
0.09	0.0071966	0.0056487	0.0043199	0.0006715	0.0000996	
0.11	0.0067257	0.0051599	0.0038158	0.0001253		
0.13	0.0061337	0.0045454	0.0031820			
0.15	0.0054021	0.0037860	0.0023988			
0.17	0.0045056	0.0028555	0.0014391			
0.19	0.0034086	0.0017169	0.0002648			
0.21	0.0020599	0.0003171				
0.23	0.0003833					
0.25						

The table 2 gives the axial velocity profile for different tapering angles at $z=4$. It is observed that axial velocity decreases towards the wall of artery. As the artery is getting widened (φ =0.02), axial velocity will be more as compared to axial velocity in less tapered artery. Also, axial velocity decreases faster as tapering angle decreases.

Table 3. Axial velocity for different Womersley numbers (α^2) at $z=4$ in converging artery

r	$\alpha^2=1$	$\alpha^2=2$	$\alpha^2=3$	$\alpha^2=4$
$R(z)$	0.1139939	0.1139939	0.1139939	0.1139939
0.01	0.0009670	0.0009668	0.0009665	0.0009661
0.03	0.0009100	0.0009099	0.0009096	0.0009092
0.05	0.0007950	0.0007949	0.0007946	0.0007943
0.07	0.0006195	0.0006194	0.0006192	0.0006190
0.09	0.0003798	0.0003798	0.0003797	0.0003796
0.11	0.0000707	0.0000706	0.0000706	0.0000706

Table 4. Axial velocity at different values of z in diverging artery

r	$z=2.5$	$z=3$	$z=4$	$z=5$	$z=6$
$R(z)$	0.238999	0.2159978	0.1939965	0.2039969	0.2459988
0.01	0.0047297	0.0037592	0.0029664	0.0033116	0.0050577
0.03	0.0046796	0.0037073	0.0029131	0.0032589	0.0050083
0.05	0.0045785	0.0036026	0.0028054	0.0031526	0.0049084
0.07	0.0044242	0.0034429	0.0026412	0.0029903	0.0047560
0.09	0.0042136	0.0032248	0.0024170	0.0027687	0.0045479
0.11	0.0039419	0.0029434	0.0021277	0.0024829	0.0042795
0.13	0.0036028	0.0025922	0.0017667	0.0021262	0.0039445
0.15	0.0031877	0.0021623	0.0013247	0.0016894	0.0035343
0.17	0.0026849	0.0016416	0.0007894	0.0011605	0.0030376
0.19	0.0020787	0.0010139	0.0001440	0.0005228	0.0024387
0.21	0.0013476	0.0002567			0.0017163
0.23	0.0004609				0.0008403

From table 3, it is found that axial velocity decreases as r increases for different values of Womersley number (α^2) at $z=4$ in converging artery (at φ =-0.01). As the Womersley number increases as axial velocity decreases slowly.

Table 4 presents the profile of axial velocity at different z in diverging artery keeping the remaining parameters constant. It also shows the radii of artery for different z at φ =0.01 It is found that axial velocity decreases as r increases irrespective of the position. It can also be observed that axial velocity decreases as the radius of artery increases.

Volumetric flow rate

The volumetric flow rate is

$$Q=\int_0^{\frac{R(z)}{R_0}} 2\pi R_0 y u(y,t)\,dy \tag{29}$$

Average volumetric flow rate is

$$Q_0=-\frac{\pi R_0^3}{8\mu_0}\left(\frac{dp}{dz}\right)_0 \tag{30}$$

where $\left(\frac{dp}{dz}\right)_0$ is the pressure gradient of blood in un-constricted uniform artery in the absence of magnetic field.

The volumetric flow rate is

$$Q=-\left[-2\pi R_0\frac{RHS}{4A}\frac{e^{jwt}}{\sum_0^\infty A_i\left(\frac{R(z)}{R_0}\right)^i}\left[\begin{array}{l}\sum_0^\infty B_i\left(\frac{R(z)}{R_0}\right)^{i+2}\sum_0^\infty A_i\frac{\left(\frac{R(z)}{R_0}\right)^{i+2}}{i+2}\\ -\sum_0^\infty A_i\left(\frac{R(z)}{R_0}\right)^{i}\sum_0^\infty B_i\frac{\left(\frac{R(z)}{R_0}\right)^{i+4}}{i+4}\end{array}\right]\right] \tag{31}$$

The non- dimensional volumetric flow rate is $\bar{Q}=\frac{Q}{Q_0}$

The following discussion will give the profiles of volumetric flow rate for a range of parameters of interest.

Table 5 exhibits the results for volumetric flow rate with axial coordinate for a range of tapering angles at $r = 0.1$. In diverging artery, as tapering angle increases, volumetric flow rate increases and in converging artery, as artery gets narrowed, volumetric flow rate decreases. The volumetric flow rate decreases as z increases from 2 to 4 and increases as z increases from 4 to 7. Volumetric flow rate is minimum at the throat of stenosis as compared to other parts of stenosis. The rate of decrease in the first half is less and rate of increase in the next half is more in diverging artery and rate of decrease is more in the first part and is less in the second half in case of converging artery.

Table 5. Volumetric flow rate for different tapering angles at $r = 0.1$

z	φ =0.02	φ =0.01	φ =-0.01	φ =-0.02
2	15.402649	10.024225	4.0255912	2.4464638
3	5.8628728	2.8513274	0.5071757	0.1683781
4	4.4289456	1.5977180	0.1010036	0.0112945
5	7.0329677	2.0919986	0.0632892	0.0023129
6	21.594366	5.8633579	0.1684850	0.0063469
7	79711.132	29.036045	1.0734561	0.0841437

A comparison of flow rate profiles for different magnetic field gradients at $r = 0.2$ in diverging artery is shown in Fig. 3. It is observed that volumetric flow rate increases with increase in magnetic field gradient. Rate of change in volumetric flow rate is less in the beginning and is more in the later part of stenosis. There is no major change in the profile of volumetric flow rate in the middle of stenosis. Hence it can be concluded that by increasing magnetic field gradient, flow rate can be increased.

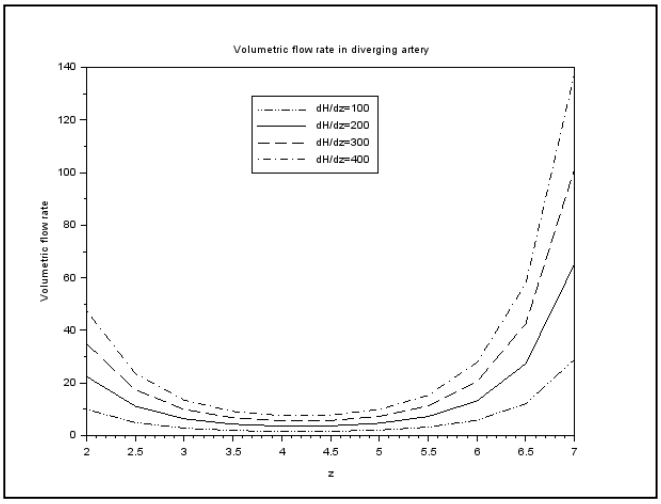

Fig. 3. Volumetric flow rate for different Womersley numbers at $r = 0.1$ in diverging artery.

It is observed from table 6 that as Womersley number (α^2) increases, axial velocity decreases slowly. This phenomenon is observed in diverging artery at $r = 0.1$ whereas the radius of non-stenosed part of artery is 0.25. It is observed that in all four cases, volumetric flow rate is in its minimum at the throat. The rate of change is less for higher values of Womersley number.

Table 6. Volumetric flow rate for different Womersley numbers at $r = 0.1$ in diverging artery

z	$\alpha^2 = 0.01$	$\alpha^2 = 0.02$	$\alpha^2 = 0.03$	$\alpha^2 = 0.06$
2	10.024223	10.024216	10.024205	10.024144
3	2.8513273	2.8513267	2.8513256	2.8513200
4	1.5977180	1.5977178	1.5977174	1.5977155
5	2.0919985	2.0919981	2.0919975	2.0919944
6	5.8633573	5.8633548	5.8633508	5.8633288
7	29.036030	29.035975	29.035882	29.035380

Volumetric flow rate at different Darcy numbers is shown in Fig. 4. It can be observed that as z increases from 2 to 5, flow rate decreases drastically and then as z increases from 5 to 7, flow

rate increases slowly. Volumetric flow rate is almost same in the middle of stenosis and attains its minimum at $z=5$ in converging artery. The profile of flow rate depends on position of stenosis and type of artery as well. It is possible to increase flow rate in the beginning and end of stenosis by increasing Darcy number.

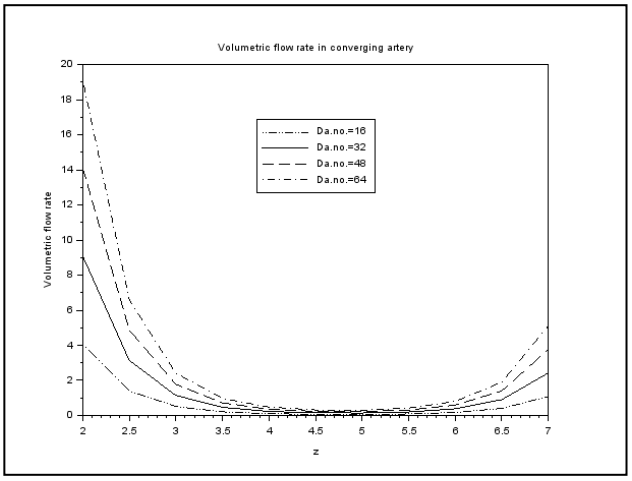

Fig. 4. Volumetric flow rate for different Darcy numbers at $r=0.0\,1$ in converging artery.

Wall shear stress

The wall shear stress is given by

$$\tau_w = \tau_0 + \left[-\mu(r) \frac{\partial u}{\partial r} \right]_{r=R(z)} \tag{32}$$

$$\tau_w = \tau_0 + \left[\mu_0 \left[1+\beta.He\left\{1-y^n\right\} \right] \frac{e^{jwt}}{R_0} \left\{ \frac{RHS}{4A} \left[\begin{array}{l} \sum_0^\infty B_i \left(\frac{R(z)}{R_0} \right)^{i+2} \sum_0^\infty iA_i \left(\frac{R(z)}{R_0} \right)^{i-1} \\ -\sum_0^\infty A_i \left(\frac{R(z)}{R_0} \right)^{i} \sum_0^\infty (i+2) B_i \left(\frac{R(z)}{R_0} \right)^{i+1} \end{array} \right] \right\} \right] \Bigg/ \left[\sum_0^\infty A_i \left(\frac{R(z)}{R_0} \right)^{i} \right] \tag{33}$$

If τ_{w0} is the wall shear stress in non-stenosed non-tapered part of artery in the absence of magnetic field, then

$$\tau_{w0} = -\frac{R_0}{2} \left(\frac{dp}{dz} \right)_0 \tag{34}$$

So, non-dimensional form of wall shear stress is $\tau = \frac{\tau_w}{\tau_{w0}}$.

Fig. 5 shows the influence of magnetic field intensity on wall shear stress for fixed value of other parameters. As z increases from 2 to 4, wall shear stress increases slowly and as z increases from 4 to 7, wall shear stress decreases drastically in diverging artery. As magnetic field intensity increases, wall shear stress decreases.

The variation in wall shear stress with z for different values of pressure gradient in converging artery is given in table 7. Wall shear increases drastically in the first part of stenosis and then decreases slowly. The same phenomena is observed for all values of pressure gradient, however the rate of change may be different. It is also observed that as pressure gradient increases, shear stress increases.

It is noticed from table 8 that as z increases from 2 to 5, wall shear stress increases and then it decreases in the converging artery in all cases of Womersley number. No considerable change in wall shear stress with respect to Womersley number is observed, however as Womersley number increases, wall shear stress decreases slightly at z = 2 and increases slightly for z >=3.

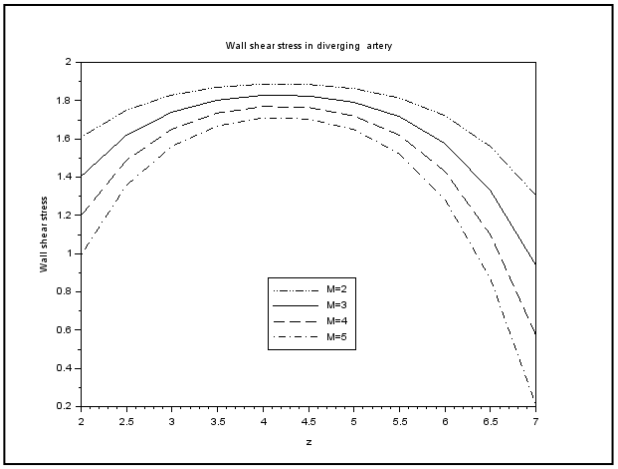

Fig. 5. Wall shear stress for different values of magnetic intensity in diverging artery.

Table 7. Wall shear stress for different pressure gradients in converging artery

Z	$\frac{\partial p}{\partial z}=10$	$\frac{\partial p}{\partial z}=20$	$\frac{\partial p}{\partial z}=30$	$\frac{\partial p}{\partial z}=40$
2	1.6702300	1.6815612	1.6928924	1.7042236
3	1.9258975	1.9284148	1.9309322	1.9334496
4	1.9777741	1.9785033	1.9792325	1.9799617
5	1.9842354	1.9847419	1.9852484	1.9857549
6	1.9674780	1.9685621	1.9696462	1.9707302
7	1.8710529	1.8754609	1.8798688	1.8842768

Table 8. Wall shear stress for different Womersley numbers in converging artery

Z	$\alpha^2=1$	$\alpha^2=2$	$\alpha^2=3$	$\alpha^2=4$
2	1.3302811	1.3302418	1.3301758	1.3300823
3	1.8503775	1.8503805	1.8503855	1.8503925
4	1.9558988	1.9558996	1.9559009	1.9559028
5	1.9690409	1.9690414	1.9690423	1.9690434
6	1.9349563	1.9349575	1.9349597	1.9349627
7	1.7388144	1.7388175	1.7388225	1.7388294

5. CONCLUSION

A pulsatile flow of blood is studied in tapered stenosed artery in the presence of externally applied transverse magnetic field with variable viscosity by assuming blood follow non-Newtonian path. In this time dependent model, Bingham plastic model – a non-Newtonian model is used to relate shear stress and shear rate. Blood viscosity is allowed to vary with radial coordinate and hematocrit. The expressions for wall shear stress, volumetric flow rate and axial velocity are obtained using Frobenius method and are found to be affected by externally magnetic field. Various combinations of parameters are used to analyze the profile of important flow characteristics. Based on the exhaustive analysis, it is found that tapering angle, viscosity and hematocrit are the important factors influencing the major characteristics of blood. Graphs are plotted to highlight the influence of different parameters on flow rate, shear stress and axial velocity. It is found that these important flow characteristics change their behavior in stenosed artery and the flow is mainly controlled by

tapering angle and significantly influenced by the strength and gradient of magnetic field. It is found that axial velocity decreases faster as tapering angle decreases and the rise in yield stress will help in elevating axial velocity.The decrease in the magnitude of velocity and wall shear stress with the increased magnetic field intensity has been observed. The effect of stenosis and yield stress reduces wall shear stress and flow rate in the presence of magnetic field. Change in the flow pattern and increase in wall shear stress are observed by treating blood as Non-Newtonian.

It is also noticed that both Darcy number and Womersley number plays important role in assessing the effect of magnetic field on important flow characteristics. As the Womersley number increases, axial velocity decreases slowly. The rate of change in volumetric flow rate is less for higher values of Womersley number. Also, it is possible to increase the flow rate in the beginning and end of stenosis by increasing Darcy number, but no considerable change in wall shear stress with respect to Womersley number is observed.

It is observed from graphs and tables that the flow can be regulated up to some extent with the help of proper combination of fluid parameters in tapered arteries and application of external transverse magnetic field with suitable pressure gradient and hematocrit level.

This study has a potential to examine the complex flow behavior of blood, under the simultaneous influence of the shape/size of stenosis and strength of externally applied magnetic field. Hence it provides a powerful tool to probe biomechanical behavior of arteries which in turn would be useful in medical field and further research.

CONFLICT OF INTERESTS

The author(s) declare that there is no conflict of interests.

REFERENCES

[1] Y. Haik, C. J. Chen, V. Pai, Magnetic fluid dynamics of blood flow, in Proceedings of the 11th ASCE Engineering Mechanics Specialty Conference, edited by Y. K. Lin and T. C. Su, Ft. Lauderdale, FL, 1996, pp. 458-461.

[2] E.E. Tzirtzilakis, N.G. Kafoussias, Mathematical models for biomagnetic fluid flow and applications, in Proceedings of 6th National Congress on Mechanics, Thessaloniki, Greece, 2001, pp. 227–232.

[3] Z. Ismail, Mathematical modeling of non-Newtonian blood flow through a tapered stenotic artery. Universiti Teknologi Malaysia Institutional Repository. 2007.

[4] B. S. Veena, Arundhati Warke, The flow behaviour of blood in two-phase time-dependent tapered stenosed artery in the presence of transverse magnetic field, J. Math. Comput. Sci. 11 (2021), 543-562.

[5] S. Chakravarty, Effects of stenosis on the flow-behaviour of blood in an artery, Int. J. Eng. Sci. 25 (1987), 1003–1016.

[6] K. Haldar, S.N. Ghosh, Effects of magnetic field on blood flow through an indented tube in the presence of erythrocytes. Indian J. Pure Appl. Math. 25(3) (1994), 345-352.

[7] J.C. Misra, S.D. Adhikary, G.C. Shit, Mathematical analysis of blood flow through an arterial segment with time‐dependent stenosis, Math. Model. Anal. 13 (2008), 401-412.

[8] M. Jain, G.C. Sharma, Singh, R. Mathematical modelling of blood flow in a stenosed artery under MHD effect through porous medium. Int. J. Eng. Trans. B. 23 (3-4) (2010), 243-251.

[9] J.C. Misra, A. Sinha, G.C. Shit, Mathematical modeling of blood flow in a porous vessel having double stenoses in the presence of an external magnetic field, Int. J. Biomath. 04 (2011), 207–225.

[10] J. Enderle, B. Susan, B. Bronzino, Introduction to Biomedical Engineering. Academic Press, London, 2005.

[11] D.K. Mandal, N.K. Manna, S. Chakrabarti, A numerical model study of steady flow through bell-shaped stenoses with and without asymmetry, Int. J. Exp. Comput. Biomech. 1 (2010), 306-331.

[12] G. Varshney, V. Katiyar, S. Kumar, Effect of magnetic field on the blood flow in artery having multiple stenosis: a numerical study. Int. J. Eng. Sci. Technol. 2(2) (2010), 967-982.

[13] M. Dabagh, P. Vasava, P. Jalali, Effects of severity and location of stenosis on the hemodynamics in human aorta and its branches, Med. Biol. Eng. Comput. 53 (2015), 463–476.

[14] Effect of Externally Applied Transverse Magnetic Field on Unsteady Flow of Blood in Tapered Stenosed Artery, Int. J. Eng. Adv. Technol. 8 (2019), 1398–1406.

[15] B.S. Veena, A.S. Warke, Study of blood flow in one half of cosine shaped stenosis in the presence of magnetic field, Int. J. Exp. Comput. Biomech. 3 (2015), 121-136.

[16] V.B. Sreenivasa, A. Suresh Warke, Study of Two-Phase Unsteady Model of Blood Flow in a Tapered Stenosed Artery in the Presence of Externally Applied Transverse Magnetic Field, in: 2018 IEEE Punecon, IEEE, Pune, India, 2018: pp. 1–7.